ChemPubSoc Europe

DOI: 10.1002/cctc.201600280

CHEMCATCHEM Communications

Mechanochemical Synthesis of Active Magnetite Nanoparticles Supported on Charcoal for Facile Synthesis of Alkynyl Selenides by C–H Activation

Balaji Mohan,[a, c] Ji Chan Park,*[b] and Kang Hyun Park*[a]

Magnetite (Fe_3O_4) nanoparticles supported on charcoal, graphene, or SBA-15 were prepared by a simple solid-state grinding technique and subsequent thermal treatment. The Fe_3O_4 nanoparticles supported on activated charcoal exhibited high catalytic activity and furnished good yields of the alkynyl selenide product in the cross-coupling reaction of diphenyl diselenide and alkynes through activation of C–H and Se–Se bonds under ecofriendly conditions, surpassing traditional copper-based catalysts to effect the same organic transformation.

Transition-metal nanoparticles (NPs) have recently gained scientific and technological interest in various areas such as sensors, fuel cells, homogeneous catalysts, and heterogeneous catalysts for important organic transformations.[1] So far, a number of solid-supported transition-metal nanoparticles, such as Cu, Au, Ru, Rh, Ir, Ni, and Pd, have been widely used as heterogeneous catalysts for important catalytic processes.[2]

In particular, iron-oxide NPs have been widely used as solid supports for the purpose of stabilizing metal nanoparticles to avoid leaching, for complete recovery by using an external magnetic field for recycling, and also to circumvent contamination with target products.[3] Owing to their low cost of preparation and the natural abundance and environmentally friendly nature of iron, the use of iron-oxide NPs themselves as catalysts for important organic reactions, such as, nitrophenol reduction, benzyl alcohol oxidation, Sonogashira coupling, borylation, and multicomponent reactions, has been reported.[4] By tuning the surface design of the support along with the size and shape of the nanoparticles, more suitable solid supports for Fe_3O_4 NPs to provide highly efficient more recyclable catalysts that are able to achieve target products at low catalyst loadings can be obtained.

Considerable efforts have been made to fabricate Fe_3O_4 NPs on various supports. Traditionally, methods used to prepare the catalysts involve multiple steps, including the preparation of the nanoparticles and their isolation, drying, and immobilization on suitable supports. However, in industry, the use of a simple method with low-costing supports is still needed, because the cost of preparing supported catalysts is important, as is the activity and reusability of the catalyst. Therefore, a facile and economical technique without any pretreatment of the solid support is desired for the synthesis of a catalyst.

Recently, solid-state grinding with subsequent infiltration of metal salts (i.e., melt–infiltration process) was utilized as a convenient and fast route to prepare supported metal catalysts owing to easy synthetic procedures, superior product crystallinity, and ease of scaling up.[5] Herein, we report an easy synthesis of iron-oxide NPs supported on activated charcoal (Fe_3O_4/C) by a facile and economic synthetic technique. To check and compare the high activity and stability of the Fe_3O_4/C catalyst in reactions for the synthesis of alkynyl selenides, other well-known supports (e.g., graphene and SBA-15) were

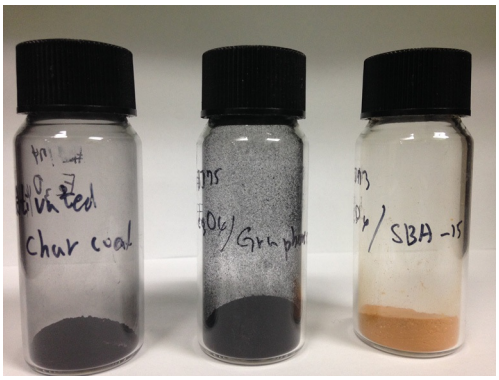

Figure 1. Pictorial representation of the Fe_3O_4 NPs on (from left to right) charcoal, single-layer graphene, and SBA-15.

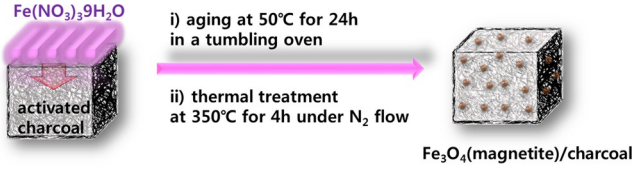

Scheme 1. Facile synthesis of Fe_3O_4/C nanocatalysts by infiltration and thermal treatment.

[a] Dr. B. Mohan, Prof. K. H. Park
Department of Chemistry and Chemistry Institute for Functional Materials
Pusan National University
Busan 609-735 (Republic of Korea)
E-mail: chemistry@pusan.ac.kr

[b] Dr. J. C. Park
Clean Fuel Laboratory
Korea Institute of Energy Research
Daejeon 305-343 (Republic of Korea)
E-mail: jcpark@kier.re.kr

[c] Dr. B. Mohan
Department of Chemistry
Madanapalle Institute of Technology & Science, Madanapalle, Chittoor
Andhra Pradesh, 305-343 (India)

Supporting Information for this article can be found under http://dx.doi.org/10.1002/cctc.201600280.

also tested. Figure 1 depicts photographs of Fe_3O_4 NPs supported on charcoal, graphene, and SBA-15.

Scheme 1 demonstrates the simple procedure for the synthesis of the Fe_3O_4/C catalyst. First, $Fe(NO_3)_3{\cdot}9H_2O$ was melt-infiltrated into the mesoporous charcoal powder by grinding at room temperature with subsequent aging at 50 °C for 24 h in a tumbling oven. Then, small magnetite nanoparticles approximately 13 nm in size were obtained by thermal decomposition of the confined salt in the carbon pores at 400 °C under nitrogen flow. The high-angle annular dark-field scanning transmission electron microscopy (HAADF-STEM) image shows bright dots, which implies incorporation of the Fe_3O_4 nanoparticles in the porous charcoal support (Figure 2a). Small Fe_3O_4 particles

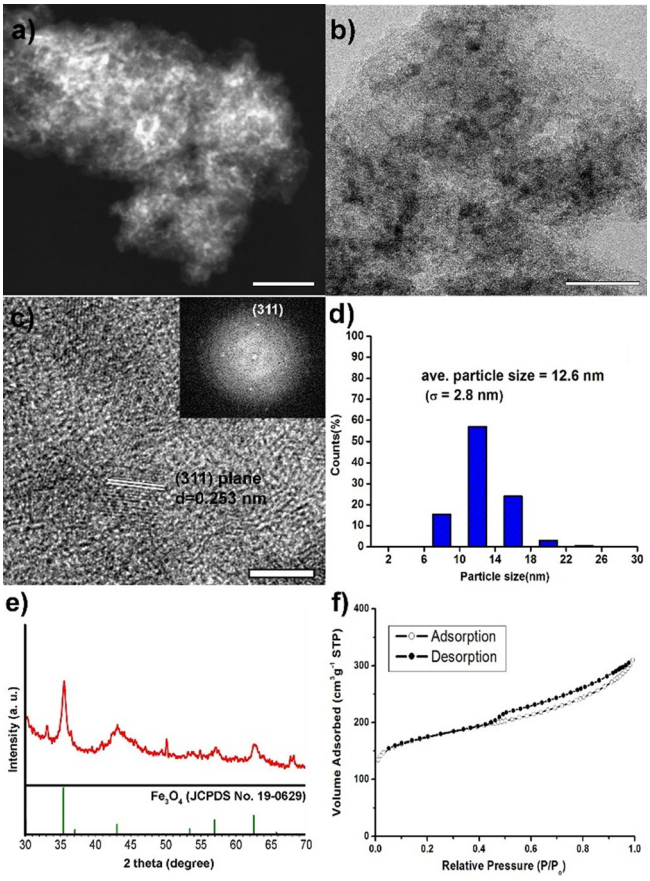

Figure 2. a) HADDF STEM image, b) low-resolution TEM image, c) HRTEM image with corresponding Fourier transform pattern (inset), d) particle-size distribution histogram, e) XRD spectrum, and f) N_2 adsorption/desorption isotherms of the Fe_3O_4/C catalyst. More than 200 particles were counted for the sample. The bars represent 100 nm (a), 50 nm (b), and 5 nm (c).

with an average diameter of 12.6 nm are observed (Figure 2b,d). High-resolution transmission electron microscopy (HRTEM) analysis revealed the lattice fringe images of the Fe_3O_4 particles, and they were measured to be $d=0.253$ nm of the (311) planes (Figure 2c). The X-ray powder diffraction (XRD) spectrum matched well with the Fe_3O_4 phase (Figure 2e, JCPDS No. 19-0629). The average size of the Fe_3O_4 nanoparticles was estimated to be 13.0 nm from the broadness of the (111) peak by the Debye–Scherrer equation. N_2 sorption experiments at −196 °C for the Fe_3O_4/C catalyst exhibited type IV adsorption/desorption hysteresis with delayed capillary evaporation at a relative pressure of 0.5 (Figure 2f). The Brunauer–Emmett–Teller (BET) surface area and total pore volume of Fe_3O_4/C were calculated to be 642 m^2g^{-1} and 0.48 cm^3g^{-1}, respectively. The size of the small pores of Fe_3O_4/C was found to be 3.9 nm, obtained from the desorption branches.

To compare the Fe_3O_4/C catalyst with other supported FeO_4 catalysts, Fe_3O_4/SBA-15 and Fe_3O_4/graphene were introduced through the same procedures. SBA-15 was chosen as a representative porous silica support with high surface area and regular pore structure. Fe_3O_4/SBA-15 showed very small nanoparticles approximately 2 nm in size (Figure 3a). HRTEM analysis revealed the lattice fringe image of the Fe_3O_4 phase, which was measured to be $d=0.21$ nm of the (400) planes (Figure 3b). In the Fe_3O_4/graphene catalyst, the particle size was less than 2 nm and, therefore, not easily detected, even by HRTEM (Figure 3c). The red circles marked in Figure 3a,c indicate extremely small nanoparticles. The lattice fringe image of the Fe_3O_4 particles was measured to be $d=0.253$ nm of the (311) planes (Figure 3d). Comparing peak intensities, the particle sizes of Fe_3O_4 in SBA-15 and graphene were much smaller than those of the Fe_3O_4/C catalyst (Figure 3e). The BET surface areas of Fe_3O_4/SBA-15 and Fe_3O_4/graphene were calculated to be 303 and 394 m^2g^{-1}, respectively (Figure 3f). The total pore volumes of Fe_3O_4/SBA-15 and Fe_3O_4/graphene were 0.88 and 1.24 cm^3g^{-1}, respectively. The Fe-loading contents of all catalysts were calculated to be approximately 10 wt% on the basis of Fe converted from the iron nitrate salt after thermal treatment.

The catalytic activity of the synthesized Fe_3O_4 NPs was tested in the cross-coupling reaction of diphenyl diselenide with alkynes to obtain the corresponding alkynyl selenides through C–H and Se–Se bond activation.

The chemistry of organochalcogens, especially selenium, has expanded rapidly over the last decade. Enormous efforts have been devoted to developing novel organochalcogen compounds for potential applications in the field of modern organic synthesis and catalysis. Organoselenium compounds are particularly attractive and have gained considerable attention among researchers, because of their ability to mimic natural compounds with important biological properties, including antiviral, antimicrobial, antitumor, and antioxidant activities.[6] Moreover, chalcogen derivatives have been applied in the development of organic materials, such as liquid crystals, organic semiconductors, and electroconductive polymers.[7] In this context, we recently developed various synthetic procedures involving the use of nanocatalysts to obtain organochalcogen derivatives. Taking into consideration our program devoted towards the synthesis of organochalcogen compounds, we turned our attention to alkynyl selenides.[8,2b]

A literature survey showed that various types of catalysts, especially copper, have been used to make C_{sp}–Se bonds through cross-coupling of either terminal alkynes or alkynyl halides with a convenient source of electron-deficient selenium[9,8a] to afford alkynyl selenides in high yields. Although

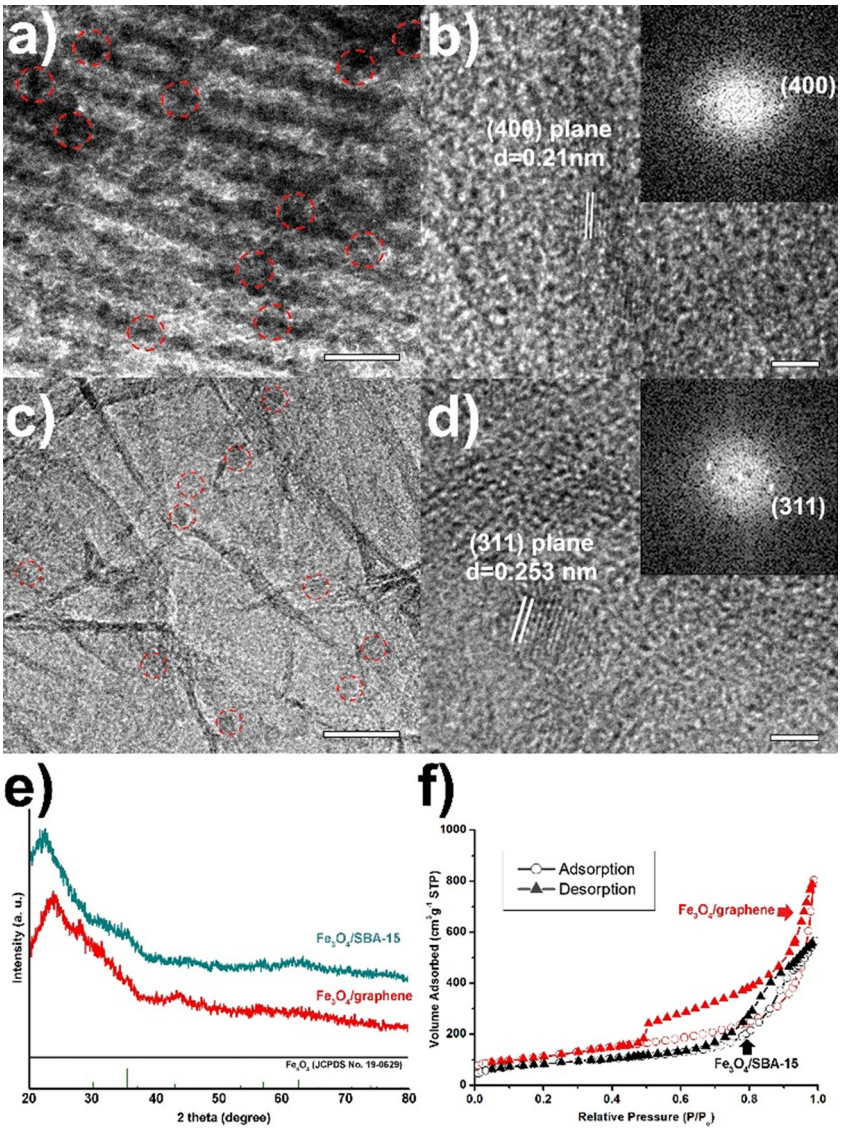

Figure 3. a) TEM and b) HRTEM images of Fe_3O_4/SBA-15 with corresponding Fourier transform pattern (inset); c) TEM and d) HRTEM images of Fe_3O_4/graphene with corresponding Fourier transform pattern (inset); e) XRD spectra and f) N_2 adsorption/desorption isotherms of Fe_3O_4/SBA-15 and Fe_3O_4/graphene. The bars represent 20 nm (a, c) and 2 nm (b, d). The red circles (a, c) indicate small nanoparticles.

rather effective, these approaches suffer from several drawbacks: 1) the preparation of alkynyl halides; 2) the requirement for phosphine- or nitrogen-based ligands; 3) the use of toxic solvents; 4) the process is homogeneous; 5) harsh reaction conditions are required; 6) environmental impact, all of which may in some cases increase the cost and limit the scope of the reaction.

In addition, most of the reported synthetic techniques use either DMSO or DMF as solvent and an oxidant to get higher yields. To overcome the aforementioned drawbacks, new and improved catalysts for this reaction are still being sought. In designing such catalysts, special consideration should be given to the cost and atom economy of the particular catalytic processes. Additionally, the choice of solvent and catalyst should be made with the consideration of environmental impact in mind.

We began our studies by examining the cross-coupling of diphenyl diselenide (**1**) and 4-ethynyltoluene (**2**) as a model reaction to optimize the experimental conditions with KO*t*Bu as the base in ethanol at 80 °C for 12 h in air. Without the aid of an additional catalyst, only 19% of **3** was observed by GC–MS analysis even after 24 h (Table 1, entry 1). We found that the addition of 0.5 mol% Fe_3O_4/C offered the product in 81% yield after 12 h (Table 1, entry 2). Decreasing the basicity resulted in an increase in the recovery of the starting materials (Table 1, entries 3–7) under identical conditions. It was also found that lowering the amount of base reduced the yield (71%; Table 1, entry 8). Surprisingly, the catalysts prepared with different supports such as SBA-15 and graphene afforded the corresponding cross-coupled products in yields of 61 and 70%, respectively. The mesoporous silica support SBA-15 may not be stable enough to completely stabilize the Fe_3O_4 NPs, especially

Table 1. Optimization of the reaction conditions.[a]

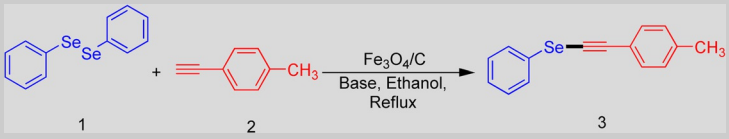

Entry	Base	Catalyst	Yield [%][b]
1	KO*t*Bu	–	19[b]
2	KO*t*Bu	Fe_3O_4/C	81 (78)[d]
3	K_2CO_3	Fe_3O_4/C	59
4	KOH	Fe_3O_4/C	73
5	K_3PO_4	Fe_3O_4/C	63
6	Na_2CO_3	Fe_3O_4/C	2
7	Cs_2CO_3	Fe_3O_4/C	64
8	KO*t*Bu	Fe_3O_4/C	71[e]
9	KO*t*Bu	Fe_3O_4/SBA 15	61[f]
10	KO*t*Bu	Fe_3O_4/graphene	70[g]

[a] Reaction conditions: **1** (1 mmol), **2** (2 mmol), base (2 mmol), catalyst (0.5 mol% with respect to **1**). [b] Determined by GC–MS. [c] In the absence of a catalyst, 24 h. [d] Yield of isolated product. [e] Reaction with base (1 equiv.). [f] 0.5 mol% Fe_3O_4/SBA-15 catalyst. [g] 0.5 mol% Fe_3O_4/graphene catalyst, 80 °C, 12 h.

Table 2. Evaluation of substrate scope.

Entry	Alkyne	Product	Yield[a] [%]
1	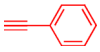	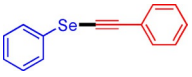	91 (89)[b]
2	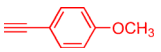	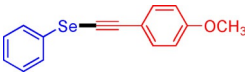	76
3	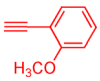		79
4	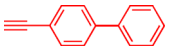	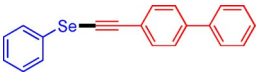	86
5	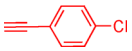	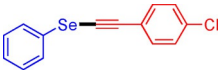	73
6		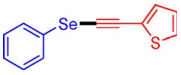	68
7	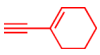	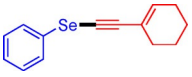	67 (61)[b]
8		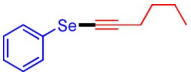	81
9	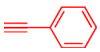	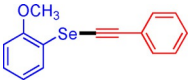	100 (96)[b]
10	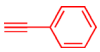	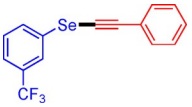	54

[a] Determined by GC–MS. [b] Yield of isolated product, 12 h.

under basic reaction conditions with high temperatures. On the other hand, carbon supports such as charcoal and graphene can be quite stable, even under strongly basic reactions. In Table 1, both Fe_3O_4/C and Fe_3O_4/graphene showed high yields (≈70–71%) for the synthesis of alkynyl selenides through activation of the C–H and Se–Se bonds by a cross-coupling process based on their small particle sizes and high surface areas and the robust framework of the support. Particularly, in terms of the efficiency relative to the price of the support, the Fe_3O_4/C catalyst among the various carbon-supported catalysts would be one of the best (commercial price: single layer graphene = 360$ per 0.5 g, activated charcoal = 107$ per 1000 g). According to our knowledge, this is the first report in which alkynyl selenides are synthesized by using ethanol as the solvent in the absence of copper, ligands, and additives with a heterogeneous catalyst loading of 0.5 mol% of Fe_3O_4 NPs under environmentally benign conditions.

On the basis of the optimized reaction conditions, we then studied the scope of this novel system for a variety of substrates. As shown in Table 2, a wide range of aryl alkynes bearing electron-donating and electron-withdrawing groups were smoothly coupled with diphenyl diselenide to give the corresponding alkynyl selenides in good to excellent yields (Table 2, entries 1–6). Aliphatic alkynes (1-ethynylcyclohexene and 1-hexyne) were also successfully coupled with diaryl diselenides with 0.5 mol% Fe_3O_4 NPs/C (Table 2, entries 7 and 8). Similarly, diaryl diselenides with methoxy and trifluoromethyl groups were tolerated by the Fe_3O_4 NPs catalyst (Table 2, entries 9 and 10).

The catalyst could be recycled efficiently five times without any significant loss of catalytic activity, as clearly shown in Figure 4; this confirmed the high stability and robustness of the heterogeneous catalytic system. These finding are very important in terms of expanding organic processes for compliance with the principles of green chemistry and sustainability.

Magnetite nanoparticles on different solid supports (e.g., activated charcoal, graphene, and SBA-15) were synthesized by using an economically feasible solid-state grinding approach followed by thermal treatment. The Fe_3O_4/C catalyst possesses remarkable catalytic efficiency for the synthesis of alkynyl selenides through activation of C–H and Se–Se bonds by a cross-coupling process. The porous-charcoal-based Fe_3O_4 catalyst was reused more than five times without prominent Fe leaching, which proved the high stability of the catalyst. The yields of the target products with challenging substituents were higher than those obtained with traditional copper catalysts, which highlights the importance of nanocatalysts.

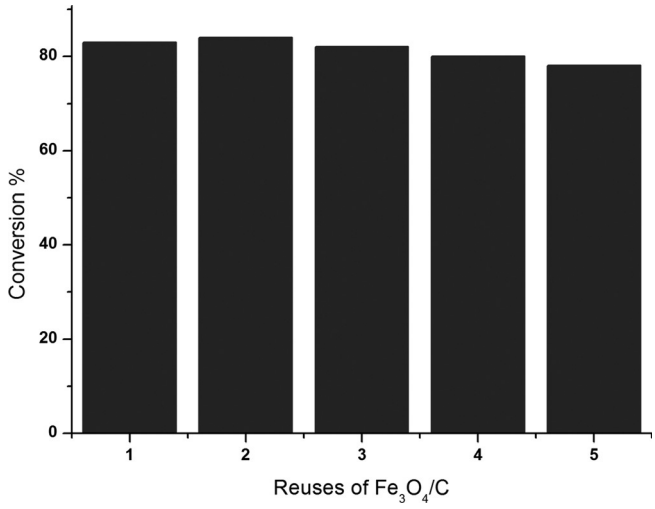

Figure 4. Recyclability of Fe_3O_4/C for the cross-coupling of diphenyl diselenide with 4-ethynyltoluene.

Experimental Section

Materials and methods

Iron nitrate nonahydrate [$Fe(NO_3)_3{\cdot}9H_2O$, ACS reagent, >98%], activated charcoal (≈100 mesh particle size, powder), Pluronic P123 (average $M_n \approx 5800$), and tetraethoxysilane (TEOS, 98%) were purchased from Sigma–Aldrich. A single-layer graphene powder was obtained from ACS Material (USA). The chemicals were used as received without further purification. ^{1}H NMR spectra were recorded with an Agilent 300 MHz spectrometer in the appropriate deuterated solvents. The chemical shift values were recorded as parts per million [ppm] relative to tetramethylsilane as an internal standard unless otherwise indicated. GC–MS spectra were recorded with a Shimadzu GC-MS spectrometer. The nature of the magnetite nanoparticles was determined by using a powder X-ray diffractometer (Rigaku D/MAX-RB 12kW). The morphology of the catalysts was measured by using a field-emission transmission electron microscope (Tecnai TF30 ST operated at 300 kV, KAIST). The surface areas for the catalysts were measured (samples were degassed in a vacuum at 300 °C for 4 h) by the BET method with a Tristar II 3020 at −196 °C.

Syntheses

SBA-15: Mesoporous silica SBA-15 was prepared by using the hydrothermal reaction method reported in the literature.[10] Typically, Pluronic P123 (16 g), distilled water (503 g), and HCl (97 g) were added into a polypropylene bottle. The mixture was stirred until Pluronic P123 was completely dissolved in the acidic solution at room temperature. After that, TEOS (34 g) was added to the solution with stirring, and the mixture was aged at 40 °C for 24 h. After aging for 24 h, the mixture was transferred into a Teflon-lined autoclave and heated at 150 °C for 24 h. The white powder was recovered through filtration, washed with water and ethanol thoroughly, and dried in air. The product was calcined at 550 °C for 5 h to produce SBA-15 with a pore diameter of 9.9 nm. The final calcined material had a surface area of 362 $m^2 g^{-1}$ and a pore volume of 1.08 $cm^3 g^{-1}$.

Fe_3O_4/C, Fe_3O_4/SBA-15, and Fe_3O_4/graphene catalysts: For the synthesis of Fe_3O_4/C, a mixture of $Fe(NO_3)_3{\cdot}9H_2O$ (0.29 g) and activated charcoal (0.5 g) in a mortar was physically ground until the color of the powder was homogeneously black. The mixture was transferred into a polypropylene bottle and aged at 50 °C in a tumbling oven for 24 h. After that, the product was cooled under an ambient atmosphere and transferred to an alumina boat in a tube-type furnace. Finally, the Fe-incorporated charcoal powder was slowly heated at a ramping rate of 2.7 °C min^{-1} up to 350 °C under a nitrogen flow of 200 mL min^{-1}. The sample was held at 350 °C for 4 h under a continuous nitrogen flow. For the preparation of the Fe_3O_4/SBA-15 and Fe_3O_4/graphene catalysts, the procedures were identical to that used for the synthesis of Fe_3O_4/C, except for the use of 0.5 g of SBA-15 and single-layer graphene as supports, respectively.

Typical procedure for the cross-coupling of alkynes and diphenyl diselenide

Diphenyl diselenide (100 mg, 0.32 mmol), phenyl acetylene (65 mg, 0.64 mmol), Fe_3O_4/C (3.7 mg, 0.5% with respect to diphenyl diselenide), base (72 mg, 0.64 mmol), and ethanol (2 mL) were added into a 10 mL aluminum-capped vial, and the mixture was stirred in a preheated oil bath maintained at 80 °C for 12 h. Then, the Fe_3O_4 NPS were filtered through a Celite bed, and the product was extracted into diethyl ether. The organic solvent was evaporated under reduced pressure. The residue was purified by column chromatography (silica gel, hexane) to afford the pure cross-coupled product. The cross-coupling reactions of other substrates were performed in a similar way.

Acknowledgements

This research was supported by the Basic Science Research Program through the National Research Foundation of Korea (NRF) funded by the Ministry of Science, ICT & Future Planning (NRF-2015R1D1A1A02060684 and NRF-2013R1A1A2012960).

Keywords: alkynes · C–H activation · mechanochemistry · nanocatalysts · supported catalysts

[1] a) A. Zhang, M. Liu, M. Liu, Y. Xiao, Z. Li, J. Chen, Y. Sun, J. Zhao, S. Fang, D. Jia, F. Li, *J. Mater. Chem. A* **2014**, *2*, 1369–1374; b) A. Zhang, Y. Tian, M. Liu, Y. Xiao, D. Jia, F. Li, *RSC Adv.* **2014**, *4*, 43973–43976; c) H. Wang, D. Wang, Z. peng, W. Tang, N. Li, F. Liu, *Chem. Commun.* **2013**, *49*, 5568–5570; d) E. Antolini, *ChemPlusChem* **2014**, *79*, 765–775; e) K. Zhang, F. Ren, H. Wang, C. Wang, M. Zhu, Y. Du, *ChemPlusChem* **2015**, *80*, 529–535; f) B. Mohan, H. Woo, S. Jang, S. Lee, S. Park, K. H. Park, *Solid State Sci.* **2013**, *22*, 16–20; g) N. Yan, C. Xiao, Y. Kou, *Coord. Chem. Rev.* **2010**, *254*, 1179–1218.

[2] a) T. Jin, M. Yan, Y. Yamamoto, *ChemCatChem* **2012**, *4*, 1217–1229; b) B. Mohan, C. Yoon, S. Jang, K. H. Park, *ChemCatChem* **2015**, *7*, 405–412; c) P. Zhao, X, Feng, D. Huang, G. Yang, D. Astruc, *Coord. Chem. Rev.* **2015**, *287*, 114–136; d) A. Maximov, A. Zolotukhina, V. Murzin, E. Karakhanov, E. Rosenberg, *ChemCatChem* **2015**, *7*, 1197–1210; e) Y. Ma, Y. Huang, Y. Cheng, L. Wang, X. Li, *Appl. Catal. A* **2014**, *484*, 154–160; f) C. H. Campos, E. Rosenberg, J. L. G. Fierro, B. F. Urbano, B. L. Rivas, C. C. Torres, P. Reyes, *Appl. Catal. A* **2015**, *489*, 280–291; g) M. Zahmakiran, *Dalton Trans.* **2012**, *41*, 12690–12696; h) Z. Yinghuai, K. Chenyan, A. T. Peng, A. Emi, W. Monalisa, L. K. Louis, N. S. Hosmane, J. A. Maguire, *Inorg. Chem.* **2008**, *47*, 5756–5761; i) K. Vijayakrishna, K. T. P. Charan, K. Manojkumar, S. Venkatesh, N. Pothanagandhi, A. Sivaramakrishna, P. Mayuri, A. Senthil Kumar, B. Sreedhar, *ChemCatChem* **2016**, *8*, 1139–1145 ; j) H. Inokawa, T. Ichikawa, H. Miyaoka, *Appl. Catal. A* **2015**, *491*, 184–188; k) V. Polshettiwar, C. Len, A. Fihri, *Coord. Chem. Rev.* **2009**,

253, 2599 – 2626; l) A. Chen, C. Ostrom, *Chem. Rev.* **2015**, *115*, 11999 – 12044.

[3] a) C. W. Lim, I. S. Lee, *Nano Today* **2010**, *5*, 412 – 434; b) M. B. Gawande, P. S. Branco, R. S. Varma, *Chem. Soc. Rev.* **2013**, *42*, 3371; c) B. Karimi, F. Mansouri, H. M. Mirzaei, *ChemCatChem* **2015**, *7*, 1736 – 1789; d) C. Jin, Y. Wang, H. Wei, H. Tang, X. Liu, T. Lu, J. Wang, *J. Mater. Chem. A* **2014**, *2*, 11202 – 11208.

[4] a) L. Li, J. Lv, Y. Shen, X. Guo, L. Peng, Z. Xie, W. Ding, *ACS Catal.* **2014**, *4*, 2746 – 2752; b) J. Deng, L. P. Mo, F. Y. Zhao, Z. H. Zhang, S. X. Liu, *ACS Comb. Sci.* **2012**, *14*, 335 – 341; c) T. Zeng, W. W. Chen, C. M. Cirtiu, A. Moores, G. Song, C. J. Li, *Green Chem.* **2010**, *12*, 570 – 573; d) M. R. Nabid, Y. Bide, M. Niknezhad, *ChemCatChem* **2014**, *6*, 538 – 546; e) H. Firouzabadi, N. Iranpoor, M. Gholinejad, J. Hoseini, *Adv. Synth. Catal.* **2011**, *353*, 125 – 132; f) G. Yan, Y. Jiang, C. Kuang, S. Wang, H. Liu, Y. Zhang, J. Wang, *Chem. Commun.* **2010**, *46*, 3170 – 3172; g) S. Kim, E. Kim, B. M. Kim, *Chem. Asian J.* **2011**, *6*, 1921 – 1925.

[5] a) G. Gorrasi, A. Sorrentino, *Green Chem.* **2015**, *17*, 2610 – 2625; b) E. Boldyreva, *Chem. Soc. Rev.* **2013**, *42*, 7719 – 7738; c) K. Ralphs, C. Hardacre, S. L. James, *Chem. Soc. Rev.* **2013**, *42*, 7701 – 7718; d) V. Safarifard, A. Morsali, *CrystEngComm* **2012**, *14*, 5130 – 5132; e) L. Li, X. Guo, F. Hao, X. Zhang, J. Chen, *New J. Chem.* **2015**, *39*, 4731 – 4736.

[6] a) G. Mugesh, W. W. Du Mont, H. Sies, *Chem. Rev.* **2001**, *101*, 2125 – 2180; b) C. W. Nogueira, G. Zeni, J. B. T. Rocha, *Chem. Rev.* **2004**, *104*, 6255 – 6286; c) V. Nascimento, N. L. Ferreira, R. F. S. Canto, K. L. Schott, E. P. Waczuk, L. Sancineto, C. Santi, J. B. T. Rocha, A. L. Braga, *Eur. J. Med. Chem.* **2014**, 87, 131 – 139.

[7] a) T. E. Frizon, J. Rafique, S. Saba, I. H. Bechtold, H. Gallardo, A. L. Braga, *Eur. J. Org. Chem.* **2015**, 3470 – 3476; b) A. Patra, Y. H. Wijsboom, G. Leitus, M. Bendikov, *Chem. Mater.* **2011**, *23*, 896 – 906; c) J. Gu, Z. A. Zhao, Y. Ding, H. L. Chen, Y. W. Zhang, C. H. Yan, *J. Am. Chem. Soc.* **2013**, *135*, 8363 – 8371; d) D. S. Rampon, F. S. Rodembusch, J. M. F. M. Schneider, I. H. Bechtold, P. F. B. Goncalves, A. A. Merlo, P. H. Schneider, *J. Mater. Chem.* **2010**, *20*, 715 – 722.

[8] a) B. Mohan, S. Hwang, H. Woo, K. H. Park, *Synthesis* **2015**, *47*, 3741 – 3745; b) B. Mohan, S. Hwang, S. Jang, K. H. Park, *Synlett* **2014**, *25*, 2078 – 2082; c) B. Mohan, S. Hwang, H. Woo, K. H. Park, *Tetrahedron* **2014**, *70*, 2699 – 2702; d) B. Mohan, K. H. Park, *Appl. Catal. A* **2016**, *519*, 78 – 84.

[9] a) E. Mohammadi, B. Movassagh, *Tetrahedron Lett.* **2014**, *55*, 1613 – 1615; b) A. Sharma, R. S. Schwab, A. L. Braga, T. Barcellos, M. W. Paixao, *Tetrahedron Lett.* **2008**, *49*, 5172 – 5174; c) L. W. Bieber, M. F. da Silva, P. H. Menezes, *Tetrahedron Lett.* **2004**, *45*, 2735 – 2737; d) M. Godoi, E. W. Ricardo, T. E. Frizon, M. S. T. Rocha, D. Singh, M. W. Paixao, A. L. Braga, *Tetrahedron* **2012**, *68*, 10426 – 10430; e) D. S. Rampon, R. Giovenardi, T. L. Silva, R. S. Rambo, A. A. Merlo, P. H. Schneider, *Eur. J. Org. Chem.* **2011**, 7066 – 7070; f) S. Ahammed, S. Bhadra, D. Kundu, B. Sreedhar, B. C. Ranu, *Tetrahedron* **2012**, *68*, 10542 – 10549.

[10] H. R. Choi, H. Woo, S. Jang, J. Y. Cheon, C. Kim, J. Park, K. H. Park, S. H. Joo, *ChemCatChem* **2012**, *4*, 1587 – 1594.

Received: March 9, 2016
Revised: April 12, 2016
Published online on June 17, 2016